Multiple isoforms of mitochondrial glutathione S-transferases and their differential induction under oxidative stress

Haider RAZA[1,2], Marie-Anne ROBIN[1], Ji-kang FANG and Narayan G. AVADHANI[3]

Department of Animal Biology and the Mari Lowe Center for Comparative Oncology, School of Veterinary Medicine, University of Pennsylvania, Philadelphia, PA 19104-6047, U.S.A.

The mitochondrial respiratory chain, which consumes approx. 85–90% of the oxygen utilized by cells, is a major source of reactive oxygen species (ROS). Mitochondrial genetic and biosynthetic systems are highly susceptible to ROS toxicity. Intramitochondrial glutathione (GSH) is a major defence against ROS. In the present study, we have investigated the nature of the glutathione S-transferase (GST) pool in mouse liver mitochondria, and have purified three distinct forms of GST: GSTA1-1 and GSTA4-4 of the Alpha family, and GSTM1-1 belonging to the Mu family. The mitochondrial localization of these multiple GSTs was confirmed using a combination of immunoblot analysis, protease protection assay, enzyme activity, N-terminal amino acid sequencing, peptide mapping and confocal immunofluorescence analysis. Additionally, exogenously added 4-hydroxynonenal (HNE), a reactive byproduct of lipid peroxidation, to COS cells differentially affected the cytosolic and mitochondrial GSH pools in a dose- and time-dependent manner. Our results show that HNE-mediated mitochondrial oxidative stress caused a decrease in the GSH pool, increased membrane lipid peroxidation, and increased levels of GSTs, glutathione peroxidase and Hsp70 (heat-shock protein 70). The HNE-induced oxidative stress persisted for longer in the mitochondrial compartment, where the recovery of GSH pool was slower than in the cytosolic compartment. Our study, for the first time, demonstrates the presence in mitochondria of multiple forms of GSTs that show molecular properties similar to those of their cytosolic counterparts. Our results suggest that mitochondrial GSTs may play an important role in defence against chemical and oxidative stress.

Key words: GSH metabolism, GST purification, 4-hydroxynonenal, lipid peroxidation, mitochondria.

INTRODUCTION

The mitochondria are an important cellular site where reactive oxygen species (ROS) are produced during respiration-coupled oxidative metabolism [1,2]. These organelles are also the direct targets of oxidative and chemical stresses that lead to mitochondrial mutations and altered gene expression [3,4]. Increased production of oxidants such as superoxides, peroxides and hydroxyl radicals could cause an imbalance in mitochondrial antioxidant defences that may result in a persistent oxidative stress. Oxidative stress has been implicated in the pathogenesis of numerous diseases, including atherosclerosis, cancer, diabetes and ischaemia/reoxygenation injury, and in alcohol- and drug-induced toxicity [1–6]. The mitochondrial glutathione (GSH) pool presents an important defence system against ROS. GSH reacts covalently with ROS, and also serves as a substrate for glutathione peroxidase (GSH-PX) and glutathione S-transferase (GST) enzymes. Mammalian mitochondria have a limited ability to synthesize GSH. The high level of GSH in mitochondria, approaching levels in the cytosol, is mainly achieved by an ATP-dependent transport of cytosolic GSH into mitochondria [7–9]. GSH conjugation of exogenous compounds, such as chemical carcinogens and drugs, and endogenous toxic metabolites such as 4-hydroxynonenal (HNE), a product of membrane lipid peroxidation (LPO) by GSTs, is generally regarded as one of the major cellular defence mechanisms against toxicity [10–14]. GSH-PX activity exhibited by GST provides protection against membrane LPO by scavenging peroxides and their end products [11–14]. Control of ROS by mitochondrial GSH and GSH-metabolizing enzymes is therefore an important mechanism for maintaining membrane integrity and ROS-induced apoptosis [15–17].

Many distinct gene families, including the Alpha, Mu, Pi, Kappa, Sigma, Theta, Zeta and Omega families, as well as over 20 distinct soluble GST isoenzymes have been identified in mammals, including humans [18,19]. The majority of GSTs are homo- or hetero-dimers of subunits of $\sim$ 26 kDa, and are found mainly in the cytosol. However, a distinct microsomal family of membrane-bound GSTs has also been reported [20,21]. Mitochondria also contain GSTs, which are believed to be similar to their cytosolic counterparts [22–24]. Mitochondrial GST 13-13, previously purified from rat liver by Harris et al. [22], has been characterized as GSTK1-1, and a human homologue hGSTK-1-1 has been identified [23]. We have previously purified a GST from mouse liver mitochondria that resembled the Alpha family [24] of GSTs. However, a detailed characterization and subunit classification of the enzyme was not carried out. We reported the

Abbreviations used: CDNB, 1-chloro-2, 4-dinitrobenzene; COX I, cytochrome oxidase subunit I; DMEM, Dulbecco's modified Eagle's medium; GSH-PX, glutathione peroxidase; GST, glutathione S-transferase; HNE, 4-hydroxynonenal; Hsp, heat-shock protein; LPO, lipid peroxidation; MALDI-TOF, matrix-assisted laser desorption ionization–time of flight; OAA, ω-octylamine agarose; ROS, reactive oxygen species; TBARS, thiobarbituric acid-reactive substances; TIM, translocase of the inner membrane.

[1] These authors contributed equally to this work.
[2] Permanent address: UAE University, Faculty of Medicine and Health Sciences, Al Ain, United Arab Emirates.
[3] To whom correspondence should be addressed (e-mail narayan@vet.upenn.edu).

presence of a GST isoform, GSTA4-4, in mitochondria of rat tissues and provided evidence for its increased expression under oxidative stress [25].

Studies on the multiplicity of GSTs and their ability to conjugate GSH with a diverse array of exogenous and endogenous compounds have helped to correlate the expression of GST isoenzymes and sensitivity to chemical toxicity under various pathophysiological conditions. The existence of a dynamic GSH pool in mitochondria and the ability of these organelles to generate metabolic intermediates from drugs and chemicals by the action of multiple mitochondrial cytochrome P450s have been reported [8,26,27]. We therefore thought that it was important to undertake a parallel study on the multiplicity of GST isoenzymes in hepatic mitochondria. In the present study we have isolated multiple forms of GST from mouse liver mitochondria and have characterized three distinct isoenzymes that belong to the Alpha and Mu families. Using COS cells as a model, we also provide evidence that the mitochondrial GSTs are induced by stress conditions, further suggesting their role in maintaining GSH homoeostasis and functioning as a defence against oxidative stress.

MATERIALS AND METHODS

Materials

HNE was purchased from Oxis Research Inc. (Portland, OR, U.S.A.). All other reagents and chemicals were purchased from Sigma Chemical Co. (St. Louis, MO, U.S.A.). Dulbecco's modified Eagle's medium (DMEM) and other cell culture reagents were obtained from Gibco Invitrogen Corp. (Grand Island, NY, U.S.A.). Polyclonal antibody against GSTA4-4 was kindly provided by Dr B. Mannervik (University of Uppsala, Sweden). Polyclonal antibody against TIM44 (translocase of the inner membrane 44) was a gift from Dr Debkumar Pain (UMDNJ, New Jersey Medical School, Newark, NJ, U.S.A.). Polyclonal antibodies against GSTA1-1 and GSTM1-1, a monoclonal antibody directed against Hsp70 (heat-shock protein of 70 kDa) and polyclonal antibody against β-actin were purchased from Oxford Biomedical Research (Oxford, MI, U.S.A.), Sigma and Santa Cruz Biotechnology (Santa Cruz, CA, U.S.A.) respectively. Reagents for SDS/PAGE and Western blot analyses were purchased from Bio-Rad Laboratories Inc. (Hercules, CA, U.S.A.).

Isolation of mouse liver mitoplasts

Male ICR mice (body weight 30 g) were purchased from Harlan Sprague Dawley Inc. (Indianapolis, IN, U.S.A.) and maintained in the Veterinary School's Animal Facility at the University of Pennsylvania. Mouse livers were homogenized in 10 vol. of sucrose/mannitol buffer and mitochondria were isolated by differential centrifugation [28]. Freshly isolated mitochondria were treated with digitonin (75 μg/mg) and resulting mitoplasts were washed two or three times to eliminate traces of digitonin, essentially as described by Bhat et al. [28]. Mitoplasts were resuspended in buffer A (50 mM potassium phosphate, pH 7.3, containing 10 % glycerol, 0.1 mM dithiothreitol, 0.1 mM EDTA and 0.1 mM PMSF) and used for further purification of the mitochondrial GST proteins. Mitoplasts contained less than 1 % microsomal contamination, as determined by assay of the microsome-specific enzyme activity NADPH:cytochrome *c* reductase (rotenone-insensitive). Potential cytosolic contamination of mitoplast preparations was assessed by a protease protection assay as described previously [24]. Proteins were measured according to the method of Lowry et al. [29].

Purification of GST from mouse liver mitoplasts

The total GST pool was purified from mouse liver mitoplasts using a combination of ω-octylamine agarose (OAA) exclusion chromatography, ammonium sulphate fractionation and GSH–agarose affinity chromatography. Mitoplasts were diluted to 5 mg/ml and sonicated in buffer A for 3 min at setting 5 of a Branson Sonifier, and proteins were solubulized for 30 min on ice by adding 1 % sodium cholate. Solubulized proteins were subjected to OAA chromatography essentially as described previously for the purification of mitochondrial cytochrome P450 [26]. GST-rich fractions, eluted in the void volume, were then subjected to ammonium sulphate fractionation. The 80 % $(NH_4)_2SO_4$ fraction was resuspended in buffer B (20 mM phosphate buffer, pH 7, 1.4 mM β-mercaptoethanol, 0.1 mM PMSF and 1 μg/l each of leupeptin, pepstatin and antipain) and dialysed overnight in the same buffer with three changes of buffer. The suspension was then applied to a GSH–agarose affinity column (10 mm × 75 mm) pre-equilibrated with buffer B. The column was washed with 5 bed volumes of buffer B supplemented with 0.2 M KCl. GSTs were eluted with buffer C (50 mM Tris/HCl, pH 9.6, 10 mM GSH, 1.4 mM β-mercaptoethanol, 0.1 mM PMSF and 1 μg/l each of leupeptin, pepstatin and antipain). GSH–agarose affinity fractions were assayed for GST activity and subjected to electrophoresis. GST-rich fractions were pooled, concentrated, dialysed against buffer B and applied to a second GSH–agarose affinity column for further purification. This time, the column was eluted successively with buffer B containing 0.2 M KCl and 5 mM GSSG, and then with 50 mM Tris/HCl, pH 9.6, containing only 5 mM GSH as described by Hiratsuka et al. [30]. Small fractions (0.2–0.5 ml) were checked for GST activity and subjected to a purity check by electrophoresis after concentration and dialysis in buffer B.

SDS/PAGE and Western blot analysis

Proteins were resolved by electrophoresis on SDS/14 %-PAGE according to the method of Laemmli [31] and visualized by Coomassie Blue staining. For Western blot analysis, proteins were transferred to nitrocellulose membranes as described by Towbin et al. [32]. After incubation with appropriate antibodies, blots were developed with the Pierce Super Signal chemiluminescence Ultra kit. Imaging and quantification were performed with a Fluor-S imager (Bio-Rad) as described previously [27].

N-terminal amino acid sequencing

The purified protein fractions F1, F2 and F3 were subjected to electrophoresis on a 14 % polyacrylamide SDS/PAGE gel and transferred to a PVDF membrane. Proteins were visualized by reversible staining with Ponceau Red, bands were excised from the membrane and N-terminal amino acid sequencing was performed by a phenylthiohydantoin-derivatization procedure in a Beckman LH 2600 gas phase sequencer.

Peptide analysis by matrix-assisted laser desorption ionization–time of flight (MALDI-TOF) MS

Purified protein fraction F2 was subjected to electrophoresis on SDS/14 %-PAGE and visualized by staining with Coomassie Blue. The major stained band was excised, and the gel slice was washed three times with 50 % acetonitrile in 200 mM NH_4HCO_3 (pH 8.0), dehydrated in 100 % acetonitrile, and dried in a vacuum

centrifuge. Gel fragments were rehydrated with a minimal volume of trypsin (10 μg/ml) solution in 40 mM NH_4HCO_3 containing 10 % acetonitrile and incubated for 12 h at 37 °C. The resultant peptides were extracted, concentrated and resuspended in 50 μl of 1 % trifluoroacetic acid/100 % acetonitrile (1:1, v/v). A fraction of each sample (1 μl) was then analysed by MS using a Voyager DE Pro instrument (Applied Biosystems, Foster City, CA, U.S.A.). Database searching using the SWISSPROT program was conducted to identify the peptide fragments from intact GST proteins.

Treatment of COS cells with oxidants and isolation of subcellular fractions

COS-7 cells were maintained in DMEM containing 10 % (v/v) fetal bovine serum and gentamicin (50 μg/ml), and incubated in a 5 % CO_2/95 % air incubator at 37 °C. Cells were grown to 60–80 % confluency and treated with various concentrations of HNE for different time intervals. HNE was dissolved in ethanol and the final concentration of ethanol in the medium was < 0.1 %. In some cases, COS cells were also treated with 100 μM H_2O_2 for 3 h. Cells harvested from eight plates (each 100 mm) were washed with PBS (pH 7.4), pooled and hand-homogenized in a Teflon fitted glass homogenizer (around 20 strokes). Mitochondrial and cytosolic fractions were prepared by differential centrifugation as described previously [27].

GSH metabolism and lipid peroxide production

GSH levels were determined in both mitochondrial and cytosolic fractions by the method of Tietze [33]. LPO in the total cell lysate and in isolated mitochondria was assayed by measuring malondialdehyde production as thiobarbituric acid-reactive substances (TBARS), as described in [34]. GST activity was assayed using 1-chloro-2,4-dinitrobenzene (CDNB) and HNE as substrates, by the procedures of Habig et al. [35] and Alin et al. [36] respectively. GSH-PX activity was determined using cumene hydroperoxide as a substrate, as described previously [37]. Glutathione reductase activity was measured according to Carlberg and Mannervik [38].

In some cases, GST activity was also measured in the presence of specific antibodies. Purified GSTs from fractions F1, F2 and F3 were preincubated with antibodies against GSTA1-1, GSTA4-4 or GSTM1-1 (10 μg of IgG/50 μg of protein) for 20 min at room temperature, and GST activity was measured using CDNB substrate as described above.

Confocal microscopy

COS-7 cells were grown on cover slips in six-well plates containing 2.0 ml of DMEM as described previously [27]. Cells were treated with HNE (25 μM) for 3 h. Cells were then fixed and permeabilized by ice-chilled methanol for 5 min, and incubated with 5 % goat serum for 1 h at room temperature to minimize nonspecific interaction of antibody. Cells were double-immunostained with a 1:100 dilution of anti-GSTA4-4 antibody and a 1:100 dilution of mouse monoclonal antibody to the mitochondrial-genome-encoded human cytochrome *c* oxidase subunit I (COX I) (Molecular Probes, Eugene, OR, U.S.A.), as a specific mitochondrial marker protein. Cells were washed three times with PBS and incubated with FITC-conjugated anti-rabbit donkey IgG for the detection of GSTA4-4, and with Alexa dye 594-conjugated anti-mouse donkey IgG for the detection of COX I. Incubations with primary and secondary antibodies were carried out at 37 °C for 1 h each. Unbound antibodies were removed by repeated washings with PBS. Fluorescence confocal microscopy was carried out under a TCS laser scanning microscope (Leica Inc. Deerfield, IL, U.S.A.) as described [27].

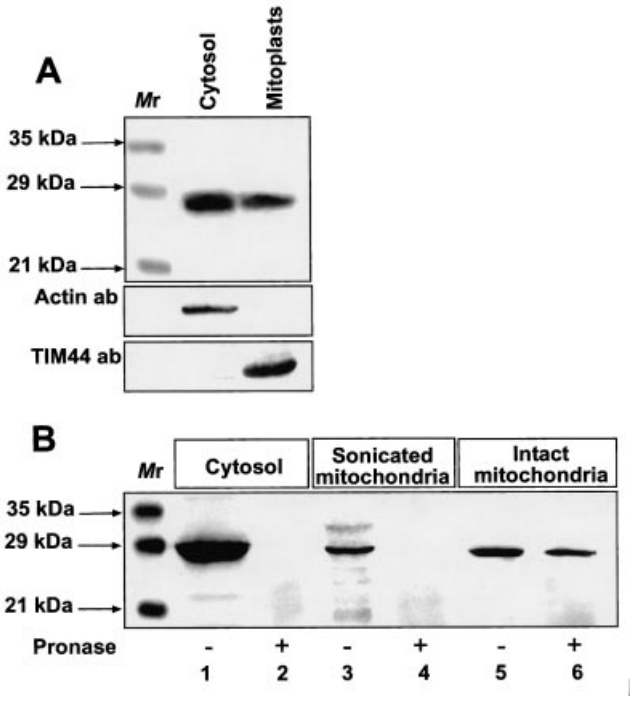

Figure 1 Mitochondrial localization and intrinsic nature of mouse liver mitochondrial GSTs

(**A**) Proteins from mouse liver cytosol (25 μg) and mitoplasts (100 μg) were resolved on SDS/14 %-PAGE and subjected to immunoblot analysis using antibodies (ab) against GSTM1-1, β-actin and TIM44 as described in the Materials and methods section. Lane M_r indicates the molecular masses of standard proteins indicated by arrows. (**B**) Mouse liver cytosol (40 μg; lanes 1 and 2) or sonicated (150 μg; lanes 3 and 4) or intact (150 μg; lanes 5 and 6) mitochondria were incubated in the presence of 20 μg of Pronase/mg of protein for 10 min on ice. After Pronase digestion, the proteins were solubulized in Laemmli sample buffer (95 °C for 5 min) and resolved on SDS/14 %-PAGE for Western blot analysis using anti-GSTM1-1 antibody as described in the Materials and methods section. Lane M_r indicates the molecular masses of standard proteins.

RESULTS

Purification of GSTs from mouse liver mitochondria

Figure 1(A) shows the immunoblot analysis of proteins from mouse liver mitoplasts and cytosol developed with an antibody to GSTM1-1. It is seen that the antibody cross-reacted with similarly migrating ($\sim$ 27 kDa) proteins from both cell fractions, although the extent of interaction with the cytosolic protein was more robust (approx. 4–5-fold more intense) compared with mitochondrial protein. Co-immunostaining of the blot also showed that the antibody to the mitochondrial inner membrane protein translocator, TIM44, interacted only with mitochondrial protein, while the antibody to cytoplasm-specific β-actin interacted exclusively with the cytosolic protein fraction. These latter results indicate the relative purity of the cell fractions used. Mitochondrial preparations used in the present study were checked routinely for purity by the above criterion and also by marker enzyme assays, which showed less than 1 % extramitochondrial contamination. To further confirm that the proteins that interacted with anti-GST antibodies from the

mitochondrial fraction were indeed localized within the inner membrane compartment, we carried out a protease protection assay with Pronase. As shown in Figure 1(B) (lanes 1 and 2), the cytoplasmic protein was readily degraded by treatment with Pronase (20 μg/mg) for 10 min on ice. The antibody-reactive GST from the mitochondrial fraction (Figure 1B, lanes 5 and 6) was relatively resistant to Pronase treatment under these conditions. Sonic disruption of the mitochondrial membrane before the addition of Pronase (lanes 3 and 4), however, rendered the protein accessible to added protease. Although not shown, antibodies to GSTA4-4 and GSTA1-1 interacted with proteins of 28 and 29 kDa from mouse liver mitoplasts. These results confirm that the antibody-reactive GSTs are indeed located inside the mitochondrial membrane compartment.

Based on these results, we attempted to purify the total mitochondrial GST pool using a combination of exclusion chromatography through OAA, $(NH_4)_2SO_4$ fractionation and affinity chromatography on GSH–agarose columns. Figure 2(A) shows the Coomassie Blue-stained gel pattern of proteins at different stages of purification. It is seen that some of the high-molecular-mass proteins (> 65 kDa) and also proteins in the range 29–39 kDa were substantially decreased during the OAA exclusion step (lanes 1 and 2). The first GSH–agarose affinity step yielded three closely migrating proteins of approx. 27–29 kDa (lane 3). The subfractions F1, F2 and F3 from the second affinity column step yielded further enrichment of individual protein species, marked 1, 2 and 3 in Figure 2(A) (lanes 4–6). The F1 fraction contained predominantly species 1, the F2 fraction contained predominantly species 2 and F3 contained predominantly species 3. The extent of purification at each of these steps, based on GST activity with CDNB as a substrate (Table 1), shows that the OAA step yielded 2.9-fold purification, while the first GSH–agarose affinity step yielded 17.5-fold purification. Fractions F1–F3 showed widely varying specific activities with CDNB as substrate, ranging from 3.0 to 11.5 μmol/min per mg, probably reflecting GST isoenzyme variations rather than the actual purity, as shown below. Direct N-terminal sequencing of the three species immobilized on a PVDF membrane (Figure 2B) showed that the slowest-migrating species 1 has an N-terminal sequence identical with that of GSTA1-1, and the fastest-migrating species 3 exhibits sequence similarity to GSTM1-1. In repeated attempts, however, the intermediate species 2 was found to have a blocked N-terminus.

With a view to firmly establishing the identity of the major antibody-reactive protein in fraction F2, we analysed the partial trypsin digests by MALDI-TOF MS analysis. As shown in Table 2 and Figure 2(C), we identified five peptides (total 56 amino acids), including the N-terminal peptide comprising residues 2–15. The peptides we recovered accounted for approx. 25% of the GSTA4-4 protein of 222 amino acids (Figure 2C), possibly due to loss of many short peptides during extraction and concentration. Although not shown, the identities of species 1 and 3 were also determined by MS-based analysis, and found to be GSTA1-1 and GSTM1-1 respectively. These results therefore indicated the presence of at least three different molecular forms of GST in the affinity-purified fractions from mouse liver mitochondria.

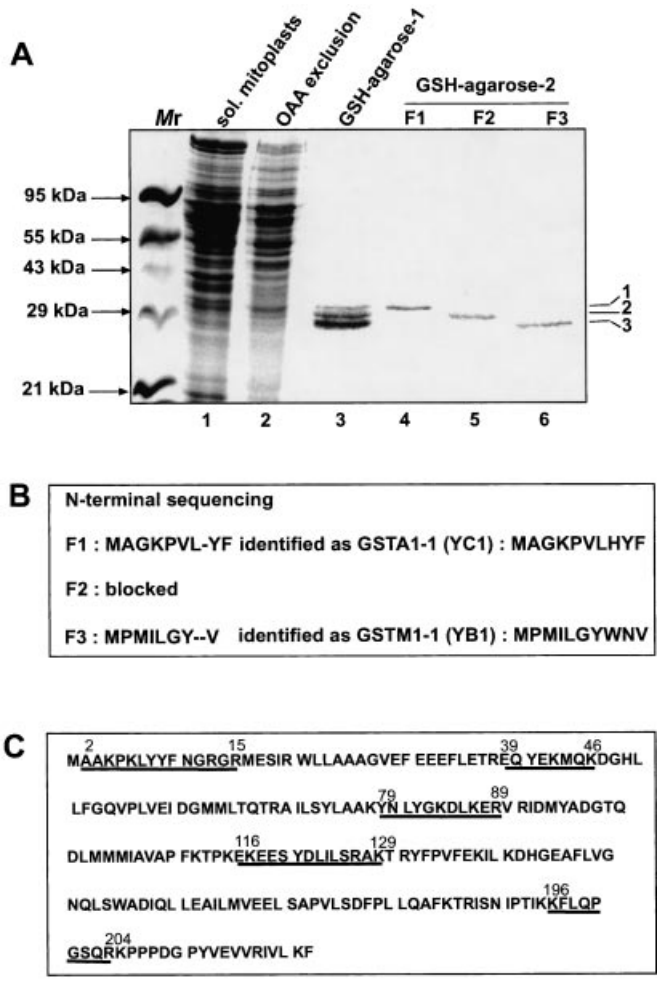

Figure 2 Characterization of multiple forms of GSTs from mouse liver mitochondria

(**A**) SDS/PAGE profile of GST purification from mouse liver. Aliquots of mouse liver mitoplast proteins at different stages of GST purification, as described in Table 1, were subjected to SDS/14%-PAGE. Protein bands were visualized by staining with Coomassie Blue. Lanes contained molecular mass standard proteins (M_r), total mitoplast proteins (40 μg; lane 1), proteins after OAA exclusion chromatography (25 μg; lane 2), eluate from the first GSH–agarose column (20 μg; lane 3), and fractions F1, F2 and F3 from the second GSH–agarose column (2 μg each; lanes 4, 5 and 6 respectively). The numbers 1, 2 and 3 on the right denote three distinct species of purified GST proteins. (**B**) N-terminal amino acid sequencing of purified GSTs. Purified proteins from fractions F1, F2 and F3 were resolved by SDS/PAGE and transferred on to PVDF membranes. N-terminal amino acid sequencing was performed as described in the text. (**C**) Amino acid sequence of mouse GSTA4-4 (SWISSPROT accession number P24472). The peptide fragments identified by MALDI-TOF MS analysis are underlined.

Immunochemical characterization and substrate preferences of mitochondrial GSTs

The nature of purified GSTs was further ascertained by immunoblotting analysis using antibodies to GSTA1-1, GSTA4-4 and GSTM1-1 (Figure 3). It should be noted that the anti-GSTA1-1 antibody also cross-reacts, though poorly, with A4-4 protein and, conversely, GSTA4-4 antibody cross-reacts with A1-1 protein [13,43], because these two isoforms belong to the same subfamily. The antibody to GSTM1-1 is, however, highly specific for this isoform. It is seen from Figure 3 that the anti-GSTA1-1 antibody interacted predominantly with a 29 kDa band and poorly with a 28 kDa band from the pooled first affinity-purified fraction. These bands co-migrate with purified species 1 and 2 from Figure 2(A). The anti-GSTA1-1 antibody interacted predominantly with purified species from fraction F1 and poorly with fraction F2, but failed to interact with fraction F3. The anti-GSTA4-4 antibody interacted with a similarly

Table 1 Purification of mouse liver GSTs

Enzyme activity during purification was monitored using CDNB as substrate. One unit of enzyme activity represents 1 μmol of substrate conjugated/min.

Fraction	Protein content (mg)	GST activity (units)	Specific activity (μmol/min per mg)	Purification (fold)	Yield (%)
Mitochondria	999	160	0.16		100
Solubilized mitoplasts	465	130	0.28	1.7	81
OAA exclusion	90	47	0.46	2.9	29
$(NH_4)_2SO_4$ fraction	68	35	0.52	3.2	22
GSH–agarose 1	8	22	2.8	17.5	14
GSH–agarose 2					
F1	1.36	7	4.9	30.6	4.2
F2	1.10	13	11.5	72	8.1
F3	0.81	2.4	3.0	18.7	1.5

Table 2 Analysis of tryptic digests of species 2 protein by MS

Protein species 2 from fraction F2 (Figure 3) was resolved by SDS/14%-PAGE, and visualized by staining with Coomassie Blue. The major band was excised, digested with trypsin and peptides were extracted as described in the Materials and methods section. The resultant peptides were analysed by MALDI-TOF MS using a Voyager DE Pro (Applied Biosystems) mass spectrometer. The mass values and predicted peptide mass analysis, residue nos. and sequence of each fragment analysed and matched with a known sequence from the data bank (SWISSPROT) are shown.

Mass (units)	Residue nos. in GSTA4-4	GSTA4-4 peptide sequence
1639.15	2–15	AAKPKLYYFNGRGR
1083.51	39–46	EQYEKMQK
1398.73	79–89	YNLYGKDLKER
1680.88	116–129	EKEESYDLILSRAK
1060.59	196–204	KFLQPGSQR

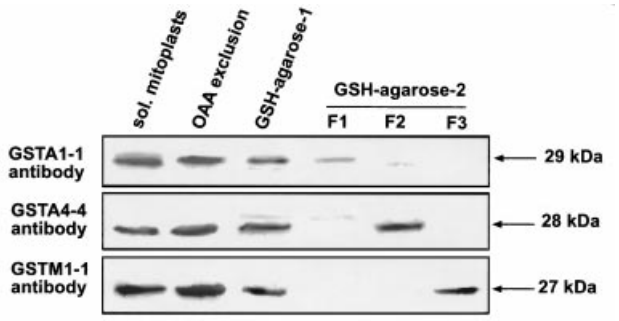

Figure 3 Reactivity of mouse liver mitochondrial GSTs with isoenzyme-specific antibodies

Proteins from solubilized (sol.) mitoplasts (40 μg), the OAA exclusion fraction (25 μg), the GST pool (10 μg) from the first GSH-affinity column and individual fractions F1, F2 and F3 (2 μg each) from the second affinity column were subjected to SDS/14%-PAGE and Western blot analysis using antibodies against GSTA1-1, GSTA4-4 and GSTM1-1. Arrows indicate the molecular masses of the major proteins characterized.

migrating protein in the total mitochondrial extract, the OAA exclusion fraction and also the first GSH-affinity fraction. The antibody interacted poorly with proteins from fraction F1 of the second GSH-affinity step, but intensely with protein in fraction F2. This antibody also did not interact with the fraction F3 protein. The anti-GSTM1-1 antibody, on the other hand, interacted with a single band (27 kDa) corresponding to species 3 (from Figure 2A). The antibody did not interact with species 1 or 2 that are predominant in fractions F1 and F2 of the second affinity purification step, but interacted with a protein co-migrating with species 3 from fraction F3. In view of the sequencing data and antibody reactivity, these results show that species 1 and 3 are GSTA1-1 and GSTM1-1 respectively. The higher cross-reactivity of species 2 with anti-GSTA4-4 further suggests that this N-terminally blocked protein is GSTA4-4.

In further attempts to characterize the differential properties of the GST forms from the three fractions, we assayed enzyme activity using CDNB, HNE and cumene hydroperoxide as substrates, and investigated the effects of the three antibodies used in Figure 3 on enzyme activity. It is seen from Table 3 that fraction F1, rich in GSTA1-1, showed moderately high specific activities of 4.7 μmol/min per mg with CDNB and 3.8 μmol/min per mg with HNE, but a relatively low peroxidase activity (0.56 μmol/min per mg) with cumene hydroperoxide. Fraction F2, rich in GSTA4-4, on the other hand showed high activities with both CDNB and HNE (10.2 and 31.5 μmol/mg respectively) and a moderately high activity of 0.96 μmol/min per mg with cumene hydroperoxide. Fraction F3, rich in GSTM1-1, showed low activities of 3.5, 1.6 and 0.14 μmol/min per mg with CDNB, HNE and cumene hydroperoxide respectively. The activity patterns with different substrates, particularly the high activity of the fraction rich in GSTA4-4 for HNE, are consistent with the reported activities of analogous GST isoenzymes from the cytosolic fraction [13,14]. Furthermore, consistent with the antibody reactivities of the three purified fractions by immunoblot analysis in Figure 3, the results of immunoinhibition of activity (Table 3) show that anti-GSTA1-1 antibody inhibited the activities towards CDNB of fractions F1 and F2 to a high level of 75–81 %, but only marginally (16 %) inhibited the activity of fraction F3. The anti-GSTA4-4 antibody yielded a similar level of inhibition. The anti-GSTM1-1 antibody, on the other hand, inhibited the activities of fractions F1 and F2 marginally (4–13 %), but the activity of fraction F3 more effectively (52 %). The antibody cross-reactivity (Figure 3) and immunoinhibition (Table 3) results are consistent with known antibody cross-reactivities among members of GST Alpha family, i.e. GSTA1-1 and GSTA4-4 [13,24].

Mitochondrial GSH metabolism during HNE-induced oxidative stress in COS cells

HNE and hydrogen peroxide (H_2O_2), products of oxidative stress in cells, are detoxified by GSTs, in particular by Alpha-class GSTs. In order to verify the role of mitochondrial GSTs and their possible role in maintaining the GSH pool, we treated COS

Table 3 Substrate specificities and immunoinhibition of GST fractions F1, F2 and F3 purified from mouse liver mitochondria

Fractions F1, F2 and F3 were assayed for GST activity using CDNB and HNE as substrates. GSH-PX activity was measured with cumene hydroperoxide as a substrate. Purified enzyme fractions were preincubated with appropriate anti-GST antibodies (10 μg of IgG/50 μg of protein) for 20 min at room temperature, and enzyme activity was measured using CDNB as substrate.

	Specific activity (μmol/min per mg)					
	CDNB					
Purified GST	No antibody	+ Anti-GSTA1-1	+ Anti-GSTA4-4	+ Anti-GSTM1-1	HNE	Cumene hydroperoxide
F1 (GSTA1-1)	4.7	0.9 (81%)	1.9 (60%)	4.5 (4%)	3.8	0.56
F2 (GSTA4-4)	10.2	2.5 (75%)	1.2 (88%)	8.9 (13%)	31.5	0.96
F3 (GSTM1-1)	3.5	2.9 (16%)	3.0 (12%)	1.7 (52%)	1.6	0.14

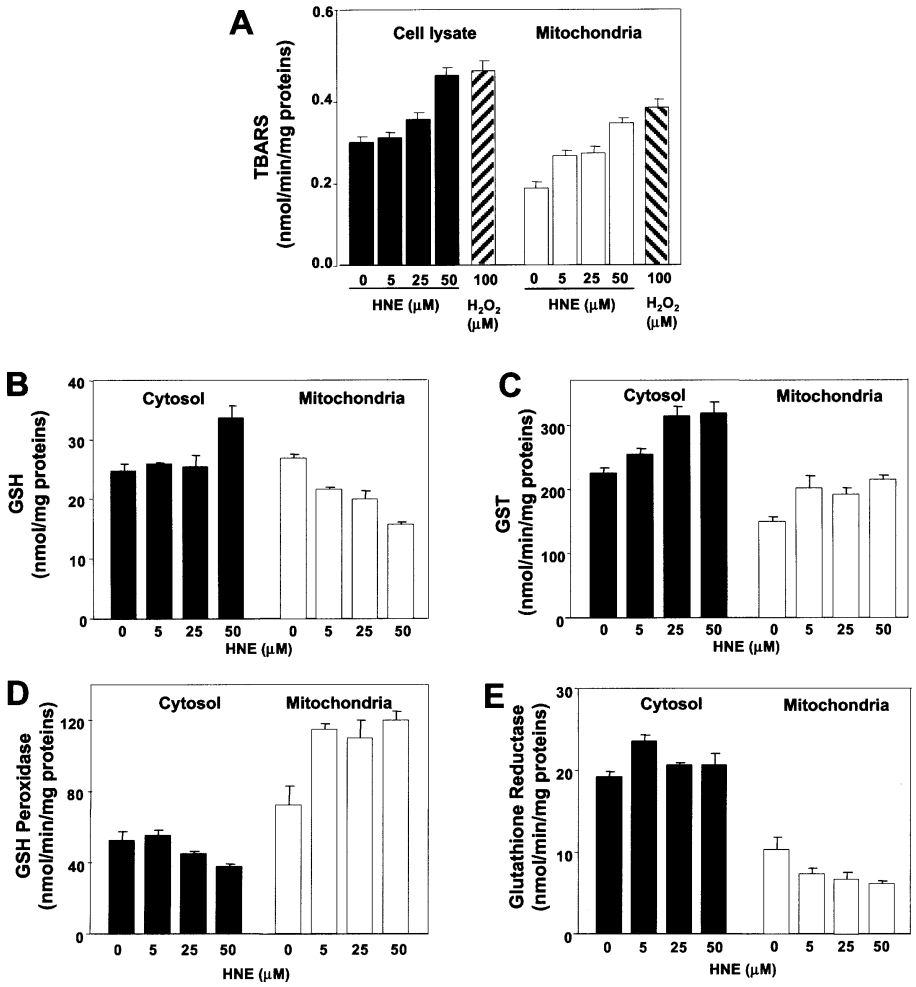

Figure 4 GSH metabolism and LPO levels in COS cell mitochondria after HNE treatment

COS cells were grown to approx. 90% confluence and treated with different concentrations of HNE (5–50 μM) or with 100 μM H_2O_2 for 3 h. Cells were harvested and subcellular fractions were isolated as described in the Materials and methods section. LPO was measured in mitochondrial and total cell lysate as malonedialdehyde formation by measuring TBARS. Cytosolic and mitochondrial GSH contents, and GST (towards CDNB), glutathione reductase and GSH-PX (towards cumene hydroperoxide) activities were measured as described in the Materials and methods section.

cells with various concentrations of HNE (5–50 μM) for different time intervals (20 min to 24 h). The extent of oxidative stress was assessed by measuring LPO, production of malonedialdehyde as TBARS, GSH concentration and levels of GSH-linked enzymes in total cell extracts and subcellular fractions (Figures 4–6). Figure 4(A) shows that treatment with various concentrations of HNE for 3 h caused a 20–50 % increase in LPO in COS cell lysates, as against a 30–80 % increase in the mitochondrial fraction. Treatment with 100 μM H_2O_2 caused a 50 % increase in LPO in the cell extract and an approx. 2-fold increase in the mitochondrial fraction. Figure 4(B) shows that treatment with up to 25 μM HNE (3 h) had no significant effect on cytosolic GSH levels, while

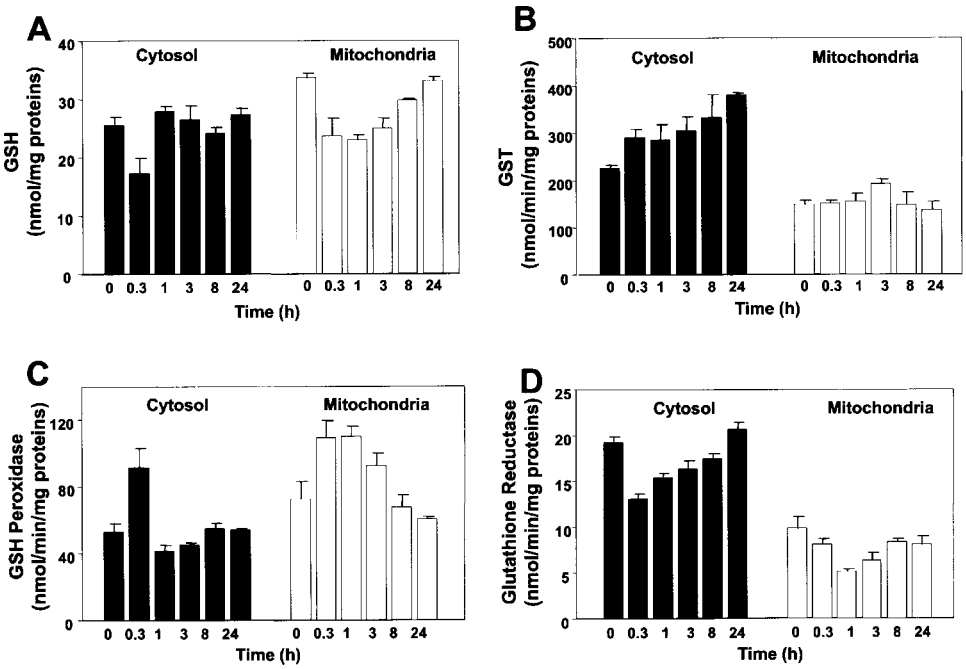

Figure 5 Mitochondrial GSH and GSH-linked enzyme levels in COS cells after treatment with HNE for various times

COS cells were treated with 25 μM HNE for different time intervals as indicated. Cytosolic and mitochondrial GSH levels and GSH-linked enzymes were determined as described in the Materials and methods section.

at a higher concentration of HNE (50 μM) the GSH level was moderately (20 %) increased. In the mitochondrial compartment, however, the GSH pool was decreased (20–50 %) with increasing levels of HNE, reaching a maximum 50 % inhibition at a concentration of 50 μM. As shown in Figure 4(C), HNE treatment resulted in a concentration-dependent increase (25–45 %) in GST activity in the both cytosol and the mitochondria. Notably, the mitochondrial fraction showed a near 2-fold increase in GSH-PX activity as compared with the cytosol (Figure 4D). Additionally, HNE treatment caused different effects in the two subcellular fractions: in the cytosol, there was a steady decline in GSH-PX activity at the higher concentrations of 25 and 50 μM HNE, while in the mitochondrial compartment there was a 50–60 % increase in activity at all concentrations of HNE used. The converse was true for glutathione reductase activity, which was marginally increased in the cytosol, whereas that in the mitochondrial fraction was decreased (20–30 %), with increasing concentrations of HNE (Figure 4E). These results show that HNE affects the GSH pool and GSH-dependent enzymes differently in the two cell compartments.

The time course of the modulation of GSH metabolism in COS cells over 24 h was studied using 25 μM HNE. Figure 5(A) shows that the cytosolic GSH pool was decreased by approx. 25 % after 20 min of treatment, followed by a rapid recovery by 1 h, which was maintained up to the 24 h tested. Although the mitochondrial GSH pool was also decreased by approx. 30–35 % by 20 min of treatment, its recovery was markedly slower, requiring nearly 24 h of growth (Figure 5A). GST activity increased steadily up to 24 h of treatment by approx. 70 % of control in the cytosol, whereas the mitochondrial GST activity was marginally increased by 3 h of treatment, only to return to the basal level by 24 h of treatment (Figure 5B). GSH-PX activity in the cytosol was increased (70 %) within 20 min of treatment, and had returned to near normal after 1 h of treatment (Figure 5C). In contrast, GSH-PX activity in the mitochondrial compartment was increased at 20 min by approx. 40 % of the control, maintained at about this level up to 3 h of treatment, and declined to near normal levels after 8 h (Figure 5C). Glutathione reductase activity in the cytosol of HNE-treated cells fell by approx. 40 % of the control value within 20 min and gradually recovered by 24 h (Figure 5D). Mitochondrial glutathione reductase activity was decreased by more than 50 % after 1 h of HNE treatment, and returned to approx. 80 % of the baseline level after 8 h of treatment (Figure 5D). Taken together, these data indicate that HNE affects the GSH pool and GSH-related enzyme activities in both the cytosol and mitochondria. However, the time courses of alterations and recovery of these processes in the two subcellular compartments vary significantly.

In a parallel study we also determined the levels of the different GST isoforms and of Hsp70, a marker of induced oxidative stress, in COS cells treated with 5–50 μM HNE and 100 μM H_2O_2 for 3 h. Figure 6(A) shows that Hsp70 was induced in both cell fractions in response to added HNE and H_2O_2. Species cross-reactive with antibodies to GSTA1-1, GSTA4-4 and GSTM1-1 which co-migrated with species 1–3 purified from mouse liver mitochondria (results not shown) were present in COS cell mitochondria also. For ease of presentation, these species, cross-reacting with the respective antibodies, will be referred to as GSTA1-1, GSTA4-4 and GSTM1-1, although their precise sequence properties and isoform classification remain unclear at the present time. It is seen that GSTA1-1 was induced in a concentration-dependent manner in the cytosolic fraction, but there was no significant induction of this isoform in the mitochondrial fraction in response to either HNE and H_2O_2. GSTA4-4 was induced in both cell fractions, with approx. 4-fold induction in mitochondria and 3-fold induction in the cytosol at 50 μM HNE. The extent of induction by H_2O_2 in the two compartments also varied. GSTM1-1 was marginally induced (1.5-fold) in both

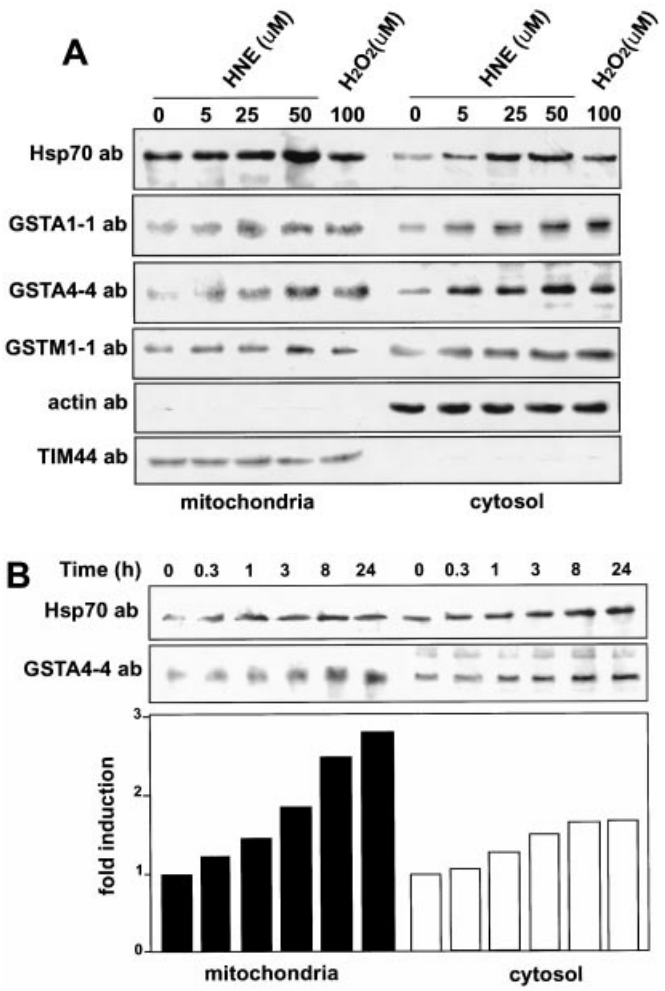

Figure 6 Steady-state levels of mitochondrial and cytosolic GSTs and Hsp70 following HNE treatment

(**A**) COS cells were treated with different concentrations of HNE (5–50 μM) or with H_2O_2 (100 μM) for 3 h. Mitochondrial (100 μg) and cytosolic (25 μg) proteins were subjected to immunoblot analysis using antibodies (ab) to Hsp70, GSTA1-1, GSTA4-4 and GSTM1-1. The blots were also probed with antibodies to β-actin and TIM44 to assess the extent of any cross-contamination. (**B**) Cells were treated with 25 μM HNE for different time intervals (0.3–24 h). Western blot analysis using antibodies to GSTA4-4 and Hsp70 was performed as described above. The blot was quantified and relative GSTA4-4 levels under the different treatment conditions are shown at the bottom.

compartments. The levels of actin and TIM44, used as loading controls and as specific markers of cytosol and mitochondria respectively, did not vary appreciably. Notably, the mitochondrial compartment did not contain a significant amount of actin, and the cytosolic fraction did not contain TIM44, demonstrating no significant cross-contamination in the cell fractions used for analysis. The time course of induction of Hsp70 and GSTA4-4 in COS cells treated with 25 μM HNE for 3 h is shown in Figure 6(B). It is seen that Hsp70 induction continued up to 8 h of treatment in both cell fractions. The results also show that maximum induction (approx. 2-fold) of cytosolic GSTA4-4 was attained within approx. 3 h, while the induction in the mitochondrial compartment (3-fold) continued up to 24 h of treatment. These results show that the overall extent of induction of GSH-linked enzymes as well as the time course of induction of the oxidative stress response varied markedly between the cytosolic and mitochondrial compartments.

Increased mitochondrial localization of GSTA4-4 by HNE treatment

Induction of GSTA4-4 by HNE treatment and the extent of mitochondrial localization under induced conditions was further verified by confocal immunofluorescence microscopy. It is seen (Figure 7) that the anti-GSTA4-4 antibody stained diffuse cytoplasmic structures, including some punctuate granular structures, which co-localized with structures stained with antibody to mitochondria-specific COX subunit I. The staining with anti-GSTA4-4 antibody was more intense in HNE-treated cells. Also, the extent of staining of membrane structures that co-localized with mitochondria-specific staining was increased substantially in HNE-treated cells. These results provide further confirmatory evidence for the presence of an HNE-inducible pool of GSTA4-4 in mitochondria.

DISCUSSION

Discrete biochemical changes in the mitochondrial compartment are thought to induce cellular apoptosis. These events include generation of ROS, release of cytochrome *c* from the mitochondrial intermembrane space, Ca^{2+} uptake, release of caspase 3, and loss of mitochondrial membrane potential [39–42]. ROS, oxidative stress and mitochondrial dysfunction have also been shown to contribute to the pathogenesis of diverse degenerative disorders [1–6]. Conjugation with GSH presents an important route for the metabolic detoxification of ROS and end products of LPO. A decrease in mitochondrial GSH levels can therefore result in the accumulation of ROS in mitochondria, leading to apoptosis and eventual cell death [12–14]. In order to better understand the mitochondrial defence mechanisms against oxidative stress, we characterized GST enzymes from mouse liver mitochondria and investigated the effects of oxidants such as HNE and H_2O_2 on the mitochondrial GSH pool and on levels of GSH-linked enzymes in COS cells.

In the present study we have identified three distinct GST isoenzymes in the GSH-affinity-purified protein fraction from the mouse liver mitochondrial matrix. We have used a number of parallel approaches to ensure that the GST pool detected both in mouse liver and in COS cell mitochondria was not due to cytosolic cross-contamination, as follows. (1) Marker enzyme assays showed that mitochondria obtained by the procedure described in the Materials and methods section contain $< 1\%$ microsome-specific contamination. (2) Immunoblot analysis showed no detectable β-actin, a cytosol-specific protein, in the mitochondrial preparations. (3) Cytosolic GST is readily degraded by digestion with Pronase, while mitochondria-associated GST is relatively resistant to protease treatment. Disruption of the mitochondrial membrane by sonication rendered the mitochondrial GSTs susceptible to protease action, suggesting that they are indeed located inside the mitochondrial inner membrane compartment. (4) Confocal immunofluorescence microscopy showed that anti-GSTA4-4 antibody stained membrane structures that co-localize with COX subunit I protein encoded by the mitochondrial genome, confirming its mitochondrial localization, and induction by HNE.

The GST pool purified from mouse liver mitochondrial matrix was resolved as three different molecular species on SDS/PAGE. The slowest migrating species (species 1) and the fastest migrating

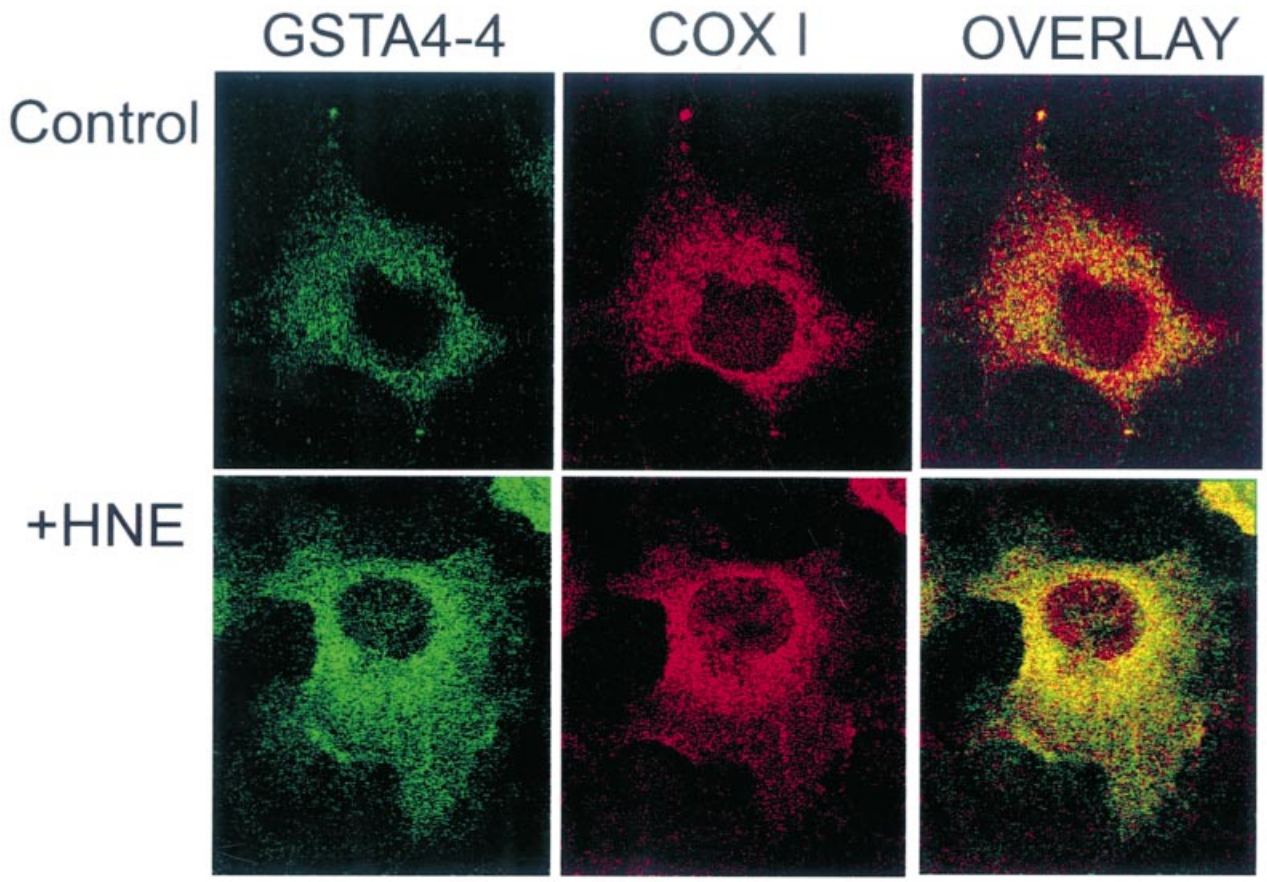

Figure 7 Localization of GSTA4-4 by confocal immunofluorescence microscopy

COS cells were grown on cover slips as described in the Materials and methods section. One set of cells was treated with 25 μM HNE for 3 h. Treated and untreated control cells were fixed, permeabilized, and stained with primary and secondary antibodies (red, anti-COX I; green, anti-GSTA4-4) as described in the Materials and methods section. The images in the right-hand panels represent overlays of GSTA4-4- and COX I-specific stains.

species (species 3) exhibited N-terminal sequences identical with those of cytosolic GSTA1-1 and GSTM1-1 respectively. Their identities were further established by cross-reactivity with antibodies against GSTA1-1 and GSTM1-1 respectively. The purified mitochondrial species 2, which cross-reacted preferentially with antibody to GSTA4-4, showed a blocked N-terminus, similar to that reported for its cytosolic counterpart [43]. However, the identity of this species as GSTA4-4 was firmly established by peptide fragment analysis by MALDI-TOF MS. Purification and characterization of GSTA1-1 and GSTA4-4 from mouse liver mitochondria thus confirmed our previous observation of the occurrence of members of the Alpha family of GSTs in the mitochondrial compartment [24,25]. All the three purified GSTs had GSH-conjugating activity with CDNB and HNE as substrates. The mitochondrial GSTs also exhibited GSH-PX activity towards cumene hydroperoxide. The cytosolic GSTA4-4 is widely regarded to be the major GST isoenzyme for the metabolic detoxification of HNE [13,14,30]. In line with these reports, mitochondrial GSTA4-4 exhibited maximum activity with HNE as substrate. Our results also show that, of the three purified mitochondrial GST isoforms, GSTA4-4 exhibited the highest GSH-PX activity (0.96 μmol/min per mg of protein).

The rates of migration of mitochondrial GSTA1-1, GSTA4-4 and GSTM1-1 on SDS/PAGE were indistinguishable from those of their cytosolic counterparts, suggesting their molecular identities. Similar to other mitochondrial GSTs reported previously [23–25], we did not observe the presence of presequences or proteolytic processing of the three isoforms purified in the present study. It is therefore likely that the mitochondrial targeting signal(s) for these GST isoforms are located within the sequences of the mature proteins. A number of mitochondria-targeted proteins, such as chaperonin 10, mitochondrial flavoprotein and isopropyl malate synthase, contain internal non-cleavable targeting sequences [23,44]. Previous studies from our laboratory demonstrated that microsome-targeted rat liver and brain cytochromes P4501A1, P4502B1 and P4502E1 are also targeted to mitochondria by virtue of their unusual N-terminal signals [27,45,46]. Those studies described a new concept of chimaeric N-terminal signals that are responsible for the bimodal targeting of proteins to mitochondria and microsomes. It is likely that, similar to that reported for P450s 2B1 and 2E1, phosphorylation or other post-translational modification activates the cryptic mitochondrial targeting signal of GST proteins. Our results are in general agreement with a recent study on the localization of GSTA4-4 in human liver mitochondria [47]. Nevertheless, in the mouse and also the rat liver, the mitochondrial GSTA4-4 pool represents only approx. 20% of the total cytoplasmic pool. A recent study [48] showed the localization of mouse GSTA4-4 to the plasma membrane, suggesting its possible role in the metabolic detoxification of membrane

peroxides generated during oxidative stress conditions. The mitochondrial targeting of these various GSTs therefore suggests a role in the metabolism of ROS and LPO products generated in the mitochondrial respiration-linked electron transport chain as well.

An important aspect of the present study relates to a possible redistribution of cytosolic and mitochondrial GST pools in COS cells under oxidative stress conditions. Oxidative stress induced by HNE and H_2O_2 caused changes in the cytosolic and mitochondrial GSH pools, and also markedly increased the levels of Hsp70, a stress marker protein, and GSTA4-4 in the mitochondrial compartment. Interestingly, we observed that treatment of COS cells with HNE affected the cytosolic and mitochondrial compartments differentially. As shown in Figures 4–6, the GSH pool and glutathione reductase enzyme activity were rapidly decreased in mitochondria and remained altered for a longer period of time. A marked increase in mitochondrial GSH-PX activity was also seen after HNE treatment. In contrast, the cytosolic GSH pool and GSH-linked enzymes were returned to near normal levels within 4–8 h after HNE treatment. The recovery of the mitochondrial GSH pool required a longer time period, suggesting a generally slow recovery from oxidative stress in this cell compartment. Increased steady-state levels of GSTs, particularly of GSTA4-4, in both the cytosol and mitochondria suggest a compensatory mechanism for detoxification of HNE. However, prolonged depletion of the GSH pool in the mitochondrial compartment after HNE treatment would indicate a delayed clearance of HNE from this organelle as compared with the cytosol. The occurrence of multiple forms of GSTs and their accumulation in mitochondria during oxidative stress conditions may suggest a defence mechanism to protect mitochondria against the deleterious effects of ROS, LPO and other oxidants.

In summary, we have purified and characterized three distinct isoenzymes of GST from mouse liver mitochondria which exhibit characteristics similar to those of their cytosolic counterparts. Using COS cells as a model system, we have shown that oxidative stress-induced alterations in the GSH pool and GSH-linked enzymes in mitochondria are persistent and prolonged compared with those in the cytosolic compartment. The occurrence of multiple forms of GST in mouse liver mitochondria suggests a role in maintaining a favourable mitochondrial redox status during cellular metabolism. Moreover, a selective modulation of GST isoenzyme levels in mitochondria may be a determinant of susceptibility to chemical and oxidative injuries.

We thank members of the Avadhani laboratory for valuable suggestions and help in the preparation of this manuscript. This work was supported in part by NIH grant GM34883-17.

REFERENCES

1 Garcia-Ruiz, C., Colell, A., Morales, A., Kaplowitz, N. and Fernandez-Checa, J. C. (1995). Role of oxidative stress generated from the mitochondrial electron transport chain and mitochondrial glutathione status in loss of mitochondrial function and activation of transcription factor nuclear factor-kappa B: studies with isolated mitochondria and rat hepatocytes. Mol. Pharmacol. **48**, 825–834

2 Shigenaga, M. K., Hagen, T. M. and Ames, B. N. (1994) Oxidative damage and mitochondrial decay in aging. Proc. Natl. Acad. Sci. U.S.A. **91**, 10771–10778

3 Zamzami, N., Marchetti, P., Castedo, M., Decaudin, D., Macho, A., Hirsch, T., Susin, S. A., Petit, P. X., Mignotte, B. and Kroemer, G. (1995) Sequential reduction of mitochondrial transmembrane potential and generation of reactive oxygen species in early programmed cell death. J. Exp. Med. **182**, 367–377

4 Goossens, V., Grooten, J., De Vos, K. and Fiers, W. (1995) Direct evidence for tumor necrosis factor-induced mitochondrial reactive oxygen intermediates and their involvement in cytotoxicity. Proc. Natl. Acad. Sci. U.S.A. **92**, 8115–8119

5 Halliwell, B. and Gutteridge, J. M. C. (1989) Free Radicals in Biology and Medicine, 2nd edn, Clarendon Press, Oxford

6 Chen, H., Carlson, E. C., Pellet, L., Moritz, J. T. and Epstein, P. N. (2001) Overexpression of metallothionein in pancreatic beta-cells reduces streptozotocin-induced DNA damage and diabetes. Diabetes **50**, 2040–2046

7 Fernandez-Checa, J. C., Yi, J. R., Garcia Ruiz, C., Ookhtens, M. and Kaplowitz, N. (1996) Plasma membrane and mitochondrial transport of hepatic reduced glutathione. Semin. Liver Dis. **16**, 147–158

8 Griffith, O. W. and Meister, A. (1985) Origin and turnover of mitochondrial glutathione. Proc. Natl. Acad. Sci. U.S.A. **82**, 4668–4672

9 Martensson, J., Lai, J. C. and Meister, A. (1990) High-affinity transport of glutathione is part of a multicomponent system essential for mitochondrial function. Proc. Natl. Acad. Sci U.S.A. **87**, 7185–7189

10 Devi, B. G. and Chan, A. W. (1996) Cocaine-induced peroxidative stress in rat liver: antioxidant enzymes and mitochondria. J. Pharmacol. Exp. Ther. **279**, 359–366

11 Uchida, K., Shiraishi, M., Naito, Y., Torii, Y., Nakamura, Y. and Osawa, T. (1999) Activation of stress signaling pathways by the end product of lipid peroxidation. 4-Hydroxy-2-nonenal is a potential inducer of intracellular peroxide production. J. Biol. Chem. **274**, 2234–2242

12 Tjalkens, R. B., Cook, L. W. and Petersen, D. R. (1999) Formation and export of the glutathione conjugate of 4-hydroxy-2,3-E-nonenal (4-HNE) in hepatoma cells. Arch. Biochem. Biophys. **361**, 113–119

13 Hubatsch, I., Ridderstrom, M. and Mannervik, B. (1998) Human glutathione transferase A4-4: an alpha class enzyme with high catalytic efficiency in the conjugation of 4-hydroxynonenal and other genotoxic products of lipid peroxidation. Biochem. J. **330**, 175–179

14 Cheng, J. Z., Singhal, S. S., Sharma, A., Saini, M., Yang, Y., Awasthi, S., Zimniak, P. and Awasthi, Y. C. (2001) Transfection of mGSTA4-4 in HL-60 cells protects against 4-hydroxynonenal-induced apoptosis by inhibiting JNK-mediated signaling. Arch. Biochem. Biophys. **392**, 197–207

15 Green, D. R. and Reed, J. C. (1998) Mitochondria and apoptosis. Science **281**, 1309–1312

16 Marchetti, P., Hirsch, T. and Zamzami, N. (1996) Mitochondrial permeability transition is a central coordinating event of apoptosis. J. Exp. Med. **184**, 1155–1160

17 Anuradha, C. D., Kanno, S. and Hirano, S. (2001) Oxidative damage to mitochondria is a preliminary step to caspase 3 activation in fluoride-induced apoptosis in HL60 cells. Free Radical Biol. Med. **31**, 367–373

18 Board, P. G., Coggan, M., Chelvanayagam, G., Easteal, S., Jermiin, L. S., Schulte, G. K., Danley, D. E., Hoth, L. R., Griffor, M. C., Kamath, A. V. et al. (2000) Identification, characterization, and crystal structure of the Omega class glutathione transferases. J. Biol. Chem. **275**, 24798–24806

19 Hayes, J. D. and Pulford, D. J. (1995) The glutathione S-transferase supergene family: regulation of GST and the contribution of the isoenzymes to cancer chemoprotection and drug resistance. CRC Crit. Rev. Biochem. Mol. Biol. **30**, 445–600

20 Prabhu, K. S., Reddy, P. V., Gumpricht, E., Hildenbrandt, G. R., Scholz, R. W., Sordillo, L. M. and Reddy, C. (2001) Microsomal glutathione S-transferase A1-1 with glutathione peroxidase activity from sheep liver: molecular cloning, expression and characterization. Biochem. J. **360**, 345–354

21 Morgenstern, R., Guthenberg, C. and Depierre, J. W. (1982) Microsomal glutathione S-transferase. Purification, initial characterization and demonstration that it is not identical to the cytosolic glutathione S-transferases A, B and C. Eur. J. Biochem. **128**, 243–248

22 Harris, J. M., Meyer, D. J., Coles, B. and Ketterer, B. (1991) A novel glutathione transferase (13-13) isolated from the matrix of rat liver mitochondria having structural similarity to class theta enzymes. Biochem. J. **278**, 137–141

23 Pemble, S. E., Wardle, A. F. and Taylor, J. B. (1996) Glutathione S-transferase class Kappa: characterization by the cloning of rat mitochondrial GST and identification of a human homologue. Biochem. J. **319**, 749–754

24 Addya, S., Mullick, J., Fang, J. K. and Avadhani, N. G. (1994) Purification and characterization of a hepatic mitochondrial glutathione S-transferase exhibiting immunochemical relationship to the alpha-class of cytosolic isoenzymes. Arch. Biochem. Biophys. **310**, 82–88

25 Bhagwat, S. V., Vijayasarathy, C., Raza, H., Mullick, J. and Avadhani, N. G. (1998) Preferential effects of nicotine and 4-(N-methyl-N-nitrosamine)-1-(3-pyridyl)-1-butanone on mitochondrial glutathione S-transferase A4-4 induction and increased oxidative stress in the rat brain. Biochem. Pharmacol. **56**, 831–839

26 Anandatheerthavarada, H. K., Addya, S., Dwivedi, R. S., Biswas, G., Mullick, J. and Avadhani, N. G. (1997) Localization of multiple forms of inducible cytochrome P450 in rat liver mitochondria: immunological characteristics and pattern of xenobiotic substrate metabolism. Arch. Biochem. Biophys. **339**, 136–150

27 Bhagwat, S. V., Biswas, G., Anandatheerthavarada, H. K., Addya, S., Pandak, W. and Avadhani, N. G. (1999) Dual targeting property of the N-terminal signal sequence of P4501A1: targeting of heterologous proteins to endoplasmic reticulum and mitochondria, J. Biol. Chem. **274**, 24014–24022

28 Bhat, N. K., Niranjan, B. G. and Avadhani, N. G. (1982) Qualitative and comparative nature of mitochondrial translation products in mammalian cells. Biochemistry **21**, 2452–2460

29 Lowry, O. H., Rosebrough, N. J., Farr, A. L. and Randall, R. J. (1951) Protein measurement with the Folin phenol reagent. J. Biol. Chem. **193**, 265–275

30 Hiratsuka, A., Saito, H., Hirose, K. and Watabe, T. (1999) Marked expression of glutathione S-transferase A4-4 detoxifying 4-hydroxy-2(E)-nonenal in the skin of rats irradiated by ultraviolet B-band light (UVB). Biochem. Biophys. Res. Commun. **260**, 740–746

31 Laemmli, U. K. (1970) Cleavage of structural proteins during the assembly of the head of bacteriophage T4. Nature (London) **227**, 680–685

32 Towbin, H., Staehelin, T. and Gordon, J. (1979) Electrophoretic transfer of proteins from polyacrylamide gels to nitrocellulose sheets: Procedure and some applications. Proc. Natl. Acad. Sci. U.S.A. **76**, 4350–4354

33 Tietze, F. (1969) Enzymatic method for quantitative determination of nanogram amounts of total and oxidized glutathione: Application to mammalian blood and other tissues. Anal. Biochem. **27**, 502–522

34 Ohkawa, H., Oshishi, N. and Yagi, K. (1979) Assay of lipidperoxides in animal tissues by thiobarbituric acid reaction. Anal. Biochem. **95**, 351–358

35 Habig, W. H., Pabst, M. J. and Jakoby, W. B. (1974) Glutathione S-transferase, the first enzymatic step in mercapturic acid formation. J. Biol. Chem. **249**, 7130–7139

36 Alin, P., Danielson, U. H. and Mannervik, B. (1985) 4-Hydroxyalk-2-enals are substrates for glutathione transferase. FEBS Lett. **179**, 267–270

37 Prohaska, J. R. and Ganther, H. E. (1977) The glutathione peroxidase activity of glutathione S-transferase. Biochem. Biophys. Res. Commun. **76**, 437–445

38 Carlberg, I. and Mannervik, B. (1985) Glutathione reductase. Methods Enzymol. **113**, 484–490

39 Richter, C., Gogvadze, V., Laffranchi, R., Schlapbach, R., Schweizer, M., Suter, M., Walter, P. and Yaffee, M. (1995) Oxidants in mitochondria: from physiology to diseases. Biochim. Biophys. Acta **1271**, 67–74

40 Mignotte, B. and Vayssiere, J. (1998) Mitochondria and apoptosis. Eur. J. Biochem. **252**, 1–15

41 Keller, J. N., Kindy, M. S., Holtsberg, F. W., St Clair, D. K., Yen, H. C., Germeyer, A., Steiner, S. M., Bruce-Keller, A. J., Hutchins, J. B. and Mattson, M. P. (1998) Mitochondrial manganese superoxide dismutase prevents neural apoptosis and reduces ischemic brain injury: suppression of peroxynitrite production, lipid peroxidation, and mitochondrial dysfunction. J. Neurosci. **18**, 687–697

42 Bossy-Wetzel, E., Newmeyer, D. D. and Green, D. R. (1998) Mitochondrial cytochrome c release in apoptosis occurs upstream of DEVD-specific caspase activation and independently of mitochondrial transmembrane depolarization. EMBO J. **17**, 37–49

43 Alin, P., Jensson, H., Cederlund, E., Jornvall, H. and Mannervik, B. (1989) Cytosolic glutathione transferases from rat liver. Primary structure of class alpha glutathione transferase 8-8 and characterization of low-abundance class Mu glutathione transferases. Biochem. J. **261**, 531–539

44 Diekert, K., Kispal, G., Guiard, B. and Lill, R. (1999) An internal targeting signal directing proteins into the mitochondrial intermembrane space. Proc. Natl. Acad. Sci. U.S.A. **96**, 11752–11757

45 Robin, M. A., Anandatheerthavarada, H. K., Fang, J. K., Cudic, M., Otvos, L. and Avadhani, N. G. (2001) Mitochondrial targeted cytochrome P450 2E1 (P450 MT5) contains an intact N terminus and requires mitochondrial specific electron transfer proteins for activity. J. Biol. Chem. **276**, 24680–24689

46 Anandatheerthavarda, H. K., Biswas, G., Mullick, J., Babu, S. V. N., Laszlo, O., Pain, D. and Avadhani, N. G. (1999) Dual targeting of cytochrome P450 2B1 to mitochondria and microsomes involves a novel signal activation by phosphorylation at Ser 128. EMBO J. **18**, 5494–5504

47 Gardner, J. L. and Gallagher, E. P. (2001) Development of a peptide antibody specific to human glutathione S-transferase alpha 4-4 (hGSTA4-4) reveals preferential localization in human liver mitochondria. Arch. Biochem. Biophys. **390**, 19–27

48 Singh, S. P., Janek, A. J., Srivastava, S. K., Awasthi, S., Awasthi, Y. C., Xia, S. J. and Zimniak, P. (2002) Membrane association of glutathione S-transferase mGSTA4-4, an enzyme that metabolizes lipid peroxidation products. J. Biol. Chem. **277**, 4232–4239

Received 4 April 2002/13 May 2002; accepted 21 May 2002
Published as BJ Immediate Publication 21 May 2002, DOI 10.1042/BJ20020533